# CONSTRUCTION OF OVERCOMPLETE MULTISCALE DICTIONARY OF SLEPIAN FUNCTIONS ON THE SPHERE

*Adeem Aslam, Student Member, IEEE and Zubair Khalid , Member, IEEE*

School of Science and Engineering, Lahore University of Management Sciences, Lahore, Pakistan
Email: adeem.aslam@uet.edu.pk, zubair.khalid@lums.edu.pk

## ABSTRACT

We construct an overcomplete and multiscale dictionary of bandlimited Slepian functions on the sphere. Slepian functions are the bandlimited eigenfunctions obtained by solving spatial-spectral concentration problem on the sphere. To this end, we develop the hierarchical equal area iso-latitude iso-longitude pixelization (HEALLPix) scheme for hierarchical partitioning of the sphere into equal area sub-regions called pixels and present its quaternary tree structure. We then solve the concentration problem of finding bandlimited functions with maximal energy concentration in the given spatial region for each pixel and use these spatially concentrated bandlimited functions as dictionary elements. We analyze the span of the dictionary elements and their mutual coherence and show that the dictionary spans the space of bandlimited functions which are optimally (energy) concentrated within a pixel on the sphere with most of its elements exhibiting negligibly small mutual coherence. Hence, the proposed dictionary is a significant tool for use in multi-resolution analysis and sparse reconstruction of signals on the sphere.

***Index Terms***— 2-sphere, spherical partitioning, spherical harmonics, spatial-spectral concentration, bandlimited signal.

## 1. INTRODUCTION

Spherical signals, which are finite energy functions defined on the sphere, arise in many areas of science and engineering including, but not limited to, computer graphics [1], wireless communication [2], acoustics [3, 4], medical imaging [5], cosmology [6], and geodesy [7]. Spherical signal processing techniques seek not only to find representations for such signals but transformations between their representations in order to store, process and reconstruct them as efficiently as possible. Signal analysis can be carried out either globally (over the whole sphere) or locally (on some region on the sphere) or over varying spatial and spectral extents. The latter is called multi-resolution analysis and has been extensively used to study time domain signals using tools such as the wavelet transform [8–10]. For signals on the sphere, the framework of wavelet analysis has started to approach maturity only recently [11–14]. Initial attempts to extend wavelet analysis to signals on sphere varied in their implementation of dilations on the sphere.

Apart from the wavelets, another way of carrying out multi-resolution analysis on the sphere is to partition the sphere into sub-regions of varying spatial extent and find basis functions for each one of them. Representing the signal in these sub-regions of varying spatial extent is similar in spirit to filtering the signal with wavelet basis of varying dilation. In the context of such multi-resolution analysis for bandlimited signals, we address the following research questions in this work:

1. How to partition the full spatial extent of the sphere into different sub-regions?
2. What basis set should be associated with each sub-region for the representation of signals?

The answer to question 1 lies in the selection of an appropriate partitioning scheme, preferably having the provision to hierarchically divide the whole sphere into different sub-regions. In Section 3, we propose one such partitioning scheme and describe its quaternary tree structure. In addressing question 2, we revert to Slepian spatial-spectral concentration problem on the sphere [15–17] which results in a set of "eigenfunctions", which not only serve as a complete basis for bandlimited signals on the sphere but also enable efficient and accurate representation of signals within different sub-regions on the sphere. Having obtained these basis functions for hierarchically partitioned sub-regions on the sphere, we store them in a bigger set, called a dictionary. This "overcomplete" dictionary of Slepian functions serves as a powerful tool for representation and reconstruction of bandlimited signals at different "scales" on the sphere. We analyze key properties of this dictionary in Section 4 before making concluding remarks in Section 5.

## 2. MATHEMATICAL PRELIMINARIES

In this section, we review the necessary mathematical background for spatial and spectral representations of spherical signals and briefly present the spatial-spectral concentration problem on the sphere.

### 2.1. Signals on 2-Sphere

We consider complex-valued signals $f(\theta, \phi)$ on the unit sphere or 2-sphere (or sphere for short), denoted by $\mathbb{S}^2$. Here $\theta \in [0, \pi]$ is the co-latitude angle measured from the positive $z$-axis and $\phi \in [0, 2\pi)$ is the longitude angle measured from the positive $x$-axis in the $x$-$y$ plane. The inner product between two such signals $f, g$ is defined as

$$\langle f, g \rangle \triangleq \int_{\mathbb{S}^2} f(\theta, \phi) \overline{g(\theta, \phi)} \sin\theta d\theta d\phi, \tag{1}$$

where $\overline{(\cdot)}$ represents the complex conjugate operation, $\sin\theta d\theta d\phi$ is the differential area element and integration is carried out over the whole sphere, i.e., $\int_{\mathbb{S}^2} \triangleq \int_{\theta=0}^{\pi} \int_{\phi=0}^{2\pi}$. Equipped with the inner product defined in (1), the set of signals on the sphere form a Hilbert space $L^2(\mathbb{S}^2)$. For a signal $f$, its energy and norm are given by $\langle f, f \rangle$ and $\|f\| \triangleq \langle f, f \rangle^{1/2}$ respectively.

Z. Khalid is supported by Pakistan HEC 2016-17 NRPU (Project no. 5925)

The Hilbert space $L^2(\mathbb{S}^2)$ is separable and its complete set of orthonormal basis functions, referred to as spherical harmonics, are defined as $Y_\ell^m(\theta,\phi) \triangleq N_\ell^m P_\ell^m(\cos\theta)e^{im\phi}$, for integer degree $\ell \geq 0$ and order[1] $|m| \leq \ell$. Here $P_\ell^m(\cos\theta)$ is the associated Legendre polynomial of degree $\ell$ and order $m$ and $N_\ell^m = \sqrt{\frac{2\ell+1}{4\pi}\frac{(\ell-m)!}{(\ell+m)!}}$ [18]. We can express any signal $f \in L^2(\mathbb{S}^2)$ as

$$f(\theta,\phi) = \sum_{\ell=0}^{\infty}\sum_{m=-\ell}^{\ell}(f)_\ell^m Y_\ell^m(\theta,\phi) = \sum_{\ell,m}^{\infty}(f)_\ell^m Y_\ell^m(\theta,\phi), \quad (2)$$

where $\sum_{\ell,m}^{\infty} \equiv \sum_{\ell=0}^{\infty}\sum_{m=-\ell}^{\ell}$ and

$$(f)_\ell^m = \langle f, Y_\ell^m\rangle = \int_{\theta=0}^{\pi}\int_{\phi=0}^{2\pi} f(\theta,\phi)\overline{Y_\ell^m(\theta,\phi)}\sin(\theta)d\theta d\phi \quad (3)$$

is the spherical harmonic coefficient of degree $\ell$ and order $m$ of the signal $f$ and constitutes its spectral domain representation. A signal is considered bandlimited to degree $L$ if $(f)_\ell^m = 0$ for $\ell, m \geq L$. Set of all such bandlimited signals on the sphere form an $L^2$-dimensional subspace of $L^2(\mathbb{S}^2)$ which is denoted by $\mathcal{H}_L$. For any signal $f \in \mathcal{H}_L$, the sum over degree in (2) is truncated at $L-1$ and its coefficients are stored in an $L^2 \times 1$ column vector as $\mathbf{f} = [(f)_0^0, (f)_1^{-1}, (f)_1^0, (f)_1^1, \ldots]^{\mathrm{T}}$, where $(\cdot)^{\mathrm{T}}$ represents the transpose operation.

### 2.2. Spatial-Spectral Concentration on the Sphere

The problem of spatial concentration of bandlimited signals (or equivalently spectral concentration of space-limited signals) was first studied in 1960s by Slepian and his co-authors [19, 20] for time domain signals, which has been extended and thoroughly investigated for multidimensional signals in the Cartesian plane [21, 22] and signals on the sphere [7, 16, 23]. To maximize the spatial energy concentration of a bandlimited signal $g \in \mathcal{H}_L$ in a region $R$, we maximize the following ratio [16]

$$\lambda = \frac{\int_R |g(\theta,\phi)|^2 \sin\theta\, d\theta\, d\phi}{\int_{\mathbb{S}^2} |g(\theta,\phi)|^2 \sin\theta\, d\theta\, d\phi} = \frac{\sum_{\ell,m}^{L-1}\overline{(g)_\ell^m}\sum_{p,q}^{L-1} K_{\ell m,pq}\,(g)_p^q}{\sum_{\ell,m}^{L-1}|g_\ell^m|^2}, \quad (4)$$

where we have used the representation of the signal in (2) in conjunction with the orthonormality of spherical harmonics on the sphere in obtaining the second equality, $\int_R$ denotes integration over the spatial region, $R$, on the sphere and

$$K_{\ell m,pq} = \int_R \overline{Y_\ell^m(\theta,\phi)}Y_p^q(\theta,\phi)\sin\theta d\theta d\phi. \quad (5)$$

Upon introducing the $L^2 \times L^2$ matrix $\mathbf{K}$ with elements $K_{\ell m,pq}$, $0 \leq \ell, p \leq L-1$, $|m| \leq \ell$, $|q| \leq p$, (4) can be equivalently expressed as

$$\lambda = \frac{\mathbf{g}^{\mathrm{H}}\mathbf{K}\mathbf{g}}{\mathbf{g}^{\mathrm{H}}\mathbf{g}}, \quad (6)$$

where $(\cdot)^{\mathrm{H}}$ represents Hermitian (conjugate) transpose and the same indexing as used for $\mathbf{g}$ is adopted for $\mathbf{K}$. Column vectors $\mathbf{g}$ which render $\lambda$ in (6) stationary are the solutions of the eigenvalue problem given by

$$\mathbf{K}\mathbf{g} = \lambda\mathbf{g}. \quad (7)$$

[1] $|\cdot|$ denotes the absolute value

The matrix $\mathbf{K}$ is Hermitian and positive definite and therefore, the eigenvectors are orthogonal (taken as orthonormal in this work) and the eigenvalues, indexed as $1 > \lambda_1 \geq \lambda_2 \geq \ldots \geq \lambda_{L^2} > 0$, are real. The eigenvalue $\lambda_\alpha$ serves as a measure of concentration of the associated eigenfunction $g_\alpha$ in the spatial region $R$. We also note that the eigenfunctions form an alternative basis for the Hilbert space $\mathcal{H}_L$ of bandlimited functions and are therefore referred to as Slepian basis.

Assuming that most of the eigenvalues in (7) are either nearly 1 (maximal concentration) or nearly 0 (minimal concentration) as investigated in detail in [16], the total number of significant eigenvalues ($\lambda_\alpha \approx 1$) is well approximated by the spherical Shannon number given by

$$N_{|R|} = \sum_{\alpha=1}^{L^2}\lambda_\alpha = \mathrm{trace}(\mathbf{K}) = \frac{|R|}{4\pi}L^2, \quad (8)$$

where $|R| = \int_R \sin\theta\, d\theta d\phi$ is the area of the region $R$. Hence, $N_{|R|}$ is a good measure of the number of well (energy) concentrated eigenfunctions in the region $R$ which in turn, essentially form a (reduced) basis set for the accurate representation of bandlimited signals concentrated in the region $R$.

## 3. CONSTRUCTION OF OVERCOMPLETE DICTIONARY

In this section, we propose to hierarchically partition the sphere into sub-regions, build the structure of an overcomplete multiscale dictionary of Slepian functions and present closed form expressions for the computation of dictionary elements over the sub-regions.

### 3.1. Hierarchical Equal Area iso-Latitude iso-Longitude Pixelization

**H**ierarchical **E**qual **A**rea iso-**L**atitude iso-**L**ongitude **Pix**elization (HEALLPix) is a hierarchical partitioning scheme of the sphere into disjoint, equal area sub-regions called pixels[2]. Number of pixels on the sphere is determined by the resolution parameter $\mathfrak{L} = 0, 1, 2, \ldots$. At $\mathfrak{L} = 0$, there is no partioning of the sphere. At $\mathfrak{L} = 1$, an iso-latitude ring at $\theta = \pi/2$ divides the whole sphere into two hemispheres and each hemisphere is further divided into two halves by iso-longitude rings at $\phi = 0, \pi$, for a total of four pixels. An increase in the resolution parameter by 1 partitions each pixel into four sub-pixels using systematic placement of iso-latitude and iso-longitude rings described below. Hence, for a given resolution level, $\mathfrak{L}$, the sphere is divided into $4^{\mathfrak{L}}$ or $2^{2\mathfrak{L}}$ disjoint pixels.

Placement of iso-Latitude Rings: An iso-latitude ring is placed at $\theta = \theta_k$ such that the spherical annulus formed by the iso-latitude rings at $\theta = \theta_{k-1}, \theta_{k+1}$ is equally divided in area. Since the area of a spherical annulus (bounded by $\theta = \theta_1, \theta_2$) is given by $A_{\theta_1,\theta_2} = 2\pi\int_{\theta_1}^{\theta_2}\sin\theta\, d\theta = 2\pi(\cos\theta_1 - \cos\theta_2)$, the condition for placement of the iso-latitude ring at $\theta = \theta_k$ becomes

$$\frac{A_{\theta_{k-1},\theta_{k+1}}}{2} = A_{\theta_k,\theta k+1} \Rightarrow z_k = \frac{z_{k-1}+z_{k+1}}{2},$$

where $z_k \equiv \cos\theta_k$. Starting with $z_0 = 1, z_1 = 0, z_2 = -1$ at $\mathfrak{L} = 1$, we find that at a given resolution level $\mathfrak{L}$, there are $2^{\mathfrak{L}} - 1$ iso-latitude rings placed at positions given by

$$z_k = \left(1 - \frac{k}{2^{\mathfrak{L}-1}}\right), \quad 1 \leq k \leq 2^{\mathfrak{L}} - 1, \quad \mathfrak{L} \geq 1, \quad (9)$$

where $z_0 = 1, z_{2^{\mathfrak{L}-1}} = 0, z_{2^{\mathfrak{L}}} = -1$.

[2] This scheme is different from the HEALPix scheme which is widely used for sampling the CMB data in cosmology and is 12 times more dense [24].

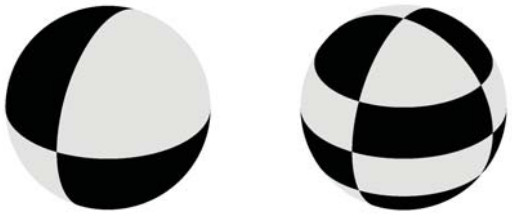

(a) $\mathfrak{L} = 1$ (b) $\mathfrak{L} = 2$

(c) $\mathfrak{L} = 3$ (d) $\mathfrak{L} = 4$

**Fig. 1**: Hierarchical Equal Area iso-Latitude iso-Longitude Pixelization of the sphere at different resolutions.

Placement of iso-Longitude Rings: Each equal area annulus is further divided into equal area pixels along $\phi$ by the iso-longitude rings. An increase in the resolution parameter by 1 divides each pixel along longitude into two halves. Hence, for a given resolution parameter, $\mathfrak{L}$, $2^{\mathfrak{L}}$ iso-longitude rings are placed at the positions given by

$$\phi_k = \frac{(k-1)\pi}{2^{\mathfrak{L}-1}}, \quad 1 \leq k \leq 2^{\mathfrak{L}}, \quad \mathfrak{L} \geq 1. \tag{10}$$

Using (9) and (10), it is trivial to show that the area of each pixel is equal to $\pi/4^{\mathfrak{L}-1}$. Pixelization of the sphere under this scheme is shown in Fig. 1 for different values of $\mathfrak{L}$.

### 3.2. Overcomplete Multiscale Dictionary of Slepian Functions

Since HEALLPix divides each pixel into four sub-pixels, it has a quaternary tree structure as shown in Fig. 2. Each node in the tree represents a pixel on the sphere. Root node of the tree, at level $h = 0$, represents the whole sphere, $\mathbb{S}^2$. Nodes at the tree level $h = 1$ represent pixels on the sphere at resolution $\mathfrak{L} = 1$. Hence, the tree level is given by $h = \mathfrak{L}$. Maximum value of $h$ is called the height of the tree and is given by $H = \mathfrak{L}_{\max}$. Nodes are labeled as $P(h, i_h)$ where $i_h$ is the index of the node at tree level $h$. Pixels at tree level $h$ are indexed 1 to $4^h$ from left to right in the tree. Hence, $1 \leq i_h \leq 4^h$ and $\bigcup_{j=4i_h-3}^{4i_h} P(h+1, j) = P(h, i_h)$, where $P(h, i_h)$ is the parent node of all the child nodes $P(h+1, j)$ at tree level $h+1$. Thus, total number of nodes in the quaternary tree, $n_P$, is given by

$$n_P = \sum_{h=0}^{H} 4^h = \frac{(4^{H+1}-1)}{3}. \tag{11}$$

Area of the pixel for a node in the tree at level $h$ is given by $|R_h| = 4^{-(h-1)}\pi = 2^{-2(h-1)}\pi$. For each node in the tree at level $h$, we solve the eigenvalue problem in (7) for the pixel represented by the node at a given bandlimit $L$ and obtain $N_{|R_h|}$ number of eigenfunctions well-concentrated in the pixel area, where

$$N_{|R_h|} = \frac{L^2}{4^h}. \tag{12}$$

We choose the tree height as $H = \lfloor \log_2 L \rfloor$ which ensures that we have at-least one well-concentrated eigenfunction for the pixels associated with the nodes at tree level $H$. Given the height, we compute $N_{|R_h|}$ number of bandlimited eigenfunctions (in the spectral domain as eigenvectors using (7)) for the pixels represented by each node of the tree at level $0 \leq h \leq H$ and store them in an $L^2 \times n_{\mathfrak{D}}$ matrix $\mathfrak{D}$, called a dictionary, as

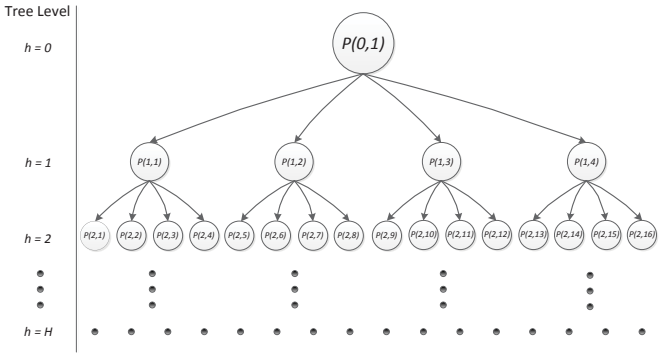


**Fig. 2**: Quaternary tree representation for HEALLPix scheme.

$$\mathfrak{D} = \left[\mathbf{d}^0_{(1,1)}, \cdots, \mathbf{d}^0_{(1,N_{|R_0|})}, \cdots, \mathbf{d}^H_{(4^H,1)}, \cdots, \mathbf{d}^H_{(4^H,N_{|R_H|})}\right] \tag{13}$$

where $n_{\mathfrak{D}} = \sum_{h=0}^{H} 4^h N_{|R_h|} = (H+1)L^2$ is the size of the dictionary and represents the total number of Slepian functions in $\mathfrak{D}$. Dictionary element $\mathbf{d}^h_{(i_h,\alpha)}$ is the $\alpha^{th}$ (spectral) eigenfunction (i.e., $\mathbf{g}_\alpha$ in (7)) for the node located at tree level $h$ and index $i_h$. Since $\mathbf{d}^h_{(i_h,\alpha)}$ for $\alpha = 1, \ldots, N_{|R_h|}$ and $1 \leq i_h \leq 4^h$ represent basis functions for all pixels at HEALLPix resolution $\mathfrak{L} = h$, it is clear from (13) that the dictionary $\mathfrak{D}$ is inherently overcomplete and multiscale in nature.

### 3.3. Computation of Slepian Functions

Every node at tree level $h$ represents a pixel at HEALLPix resolution $\mathfrak{L} = h$. As described in Section 3.1 and depicted in Fig. 1, each pixel is characterized by two co-latitude angles, $\theta_1, \theta_2$, and two longitude angles, $\phi_1, \phi_2$. To compute the Slepian functions for a pixel, we solve for the elements of matrix $\mathbf{K}$ in (5) using the formulation given in [15] as

$$K_{\ell m,pq} = \sum_{m'=-\ell}^{\ell} F^{\ell}_{m,m'} \sum_{q'=-p}^{p} F^{p}_{q,q'} Q(m'+q') S(q-m), \tag{14}$$

where $F^{\ell}_{m,m'} = i^{-m}\sqrt{\frac{2\ell+1}{4\pi}}\Delta^{\ell}_{m',m}\,\Delta^{\ell}_{m',0}$ and

$$Q(m) = \begin{cases} \frac{1}{4}(2im(\theta_2-\theta_1)) + e^{2im\theta_1} - e^{2im\theta_2}, & |m| = 1 \\ \frac{1}{m^2-1}\Big(e^{im\theta_1}(-\cos\theta_1 + im\sin\theta_1) + \\ e^{im\theta_2}(\cos\theta_2 - im\sin\theta_2)\Big), & |m| \neq 1, \end{cases}$$

$$S(m) = \begin{cases} \phi_2 - \phi_1, & m = 0 \\ \frac{i}{m}(e^{im\phi_1} - e^{im\phi_2}), & m \neq 0, \end{cases}$$

Here $\Delta^{\ell}_{m',n} \triangleq d^{\ell}_{m,n}(\pi/2)$, where $d^{\ell}_{m,n}$ are the Wigner-$d$ functions [18]. Fig. 3 shows Slepian functions, obtained using (2), for different nodes in a tree constructed for bandlimit $L = 32$ ($H = 5$).

## 4. ANALYSIS

In this section, we analyze the dictionary for two important properties, namely Range and Mutual Coherence.

### 4.1. Range of $\mathfrak{D}$

We compare the range space of $\mathfrak{D}_{h=1,1}$ which is the vector space spanned by the dictionary elements for the node $P(1,1)$, to the vec-

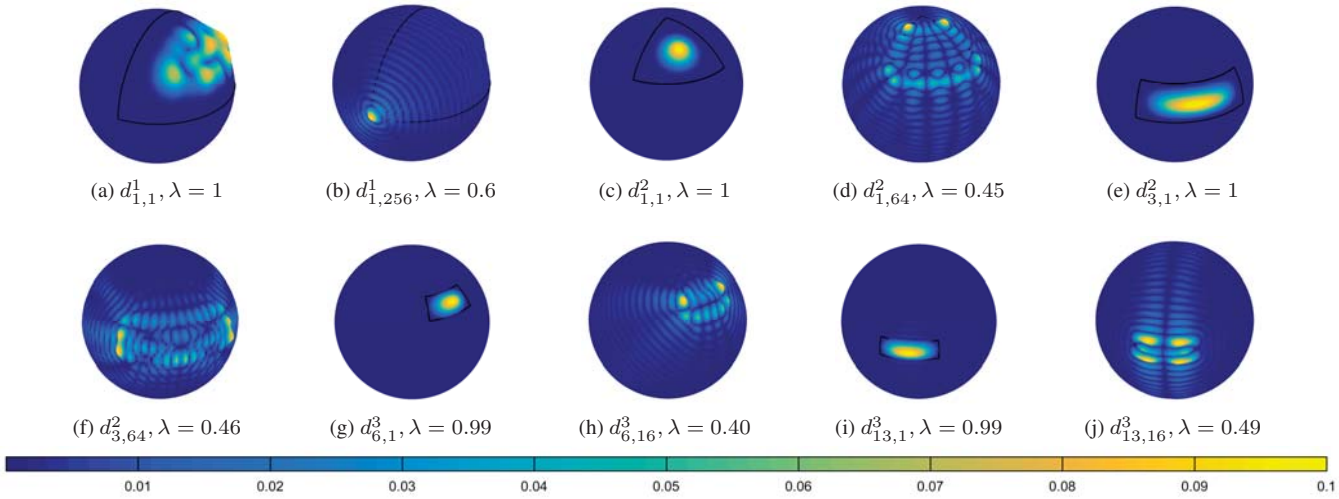


**Fig. 3**: Slepian functions for different nodes in a tree constructed for bandlimit $L = 32$ $(H = 5)$. For each node we plot the magnitude of the most (optimally) concentrated and least (optimally) concentrated Slepian functions. Boundary of the pixels is shown in black.

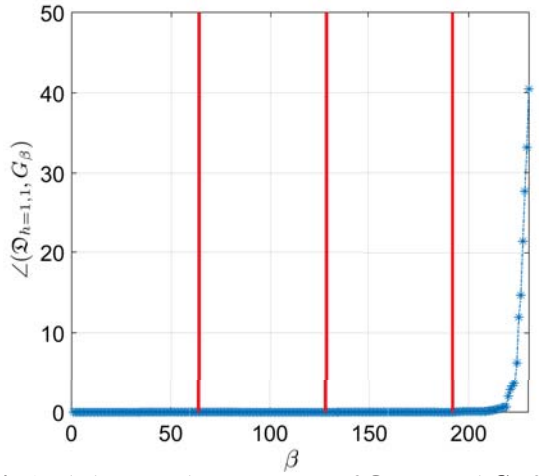


**Fig. 4**: Angle between the range space of $\mathfrak{D}_{h=1,1}$ and $G_\beta$ for different values of $\beta$ and bandlimit $L = 16$ $(H = 4)$. Thick red lines mark the integer multiples of Shannon Number, $N_{|R_1|} = 64$.

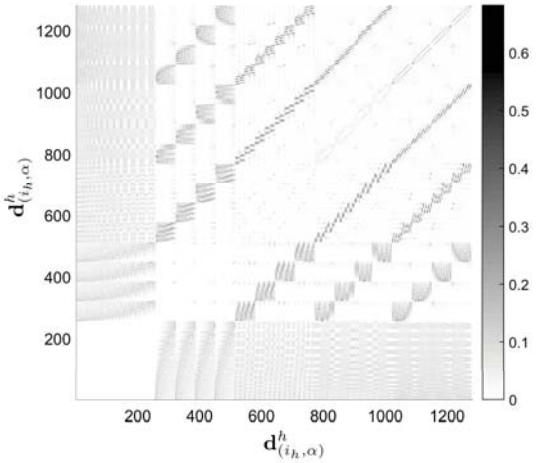


**Fig. 5**: Mutual coherence between elements of the dictionary constructed for bandlimit $L = 16$ $(H = 4)$.

tor spaces of bandlimited functions which are optimally concentrated within the pixel represented by the node $P(1, 1)$, i.e., the range space of the matrix $G_\beta = \left[\mathbf{g}_1, \mathbf{g}_2, \ldots, \mathbf{g}_\beta\right]$, $\beta = 1, 2, \ldots, N_{|R_1|}$, by investigating the angle between them. We define the maximum principle angle between two subspaces (of different dimensions in general) as the angle between them. The results are shown in Fig. 4 for bandlimit $L = 16$ and tree height $H = 4$. It can be seen that elements of the dictionary comfortably span the space of bandlimited functions optimally concentrated within pixel represented by the node $P(1, 1)$, since the angle $\angle(\mathfrak{D}_{h=1,1}, G_\beta)$ is essentially 0 for not only just the optimally concentrated eigenfunctions, i.e., $\beta \leq N_{|R_1|}$ but also for $N_{|R_1|} \leq \beta \leq 3N_{|R_1|}$.

### 4.2. Mutual Coherence between Dictionary Elements

Mutual coherence between elements of the dictionary is defined as $M = |(\mathbf{d}^h_{(i_h,\alpha)})^{\mathrm{H}}\mathbf{d}^h_{(i_h,\beta)}|$, $\alpha \neq \beta$. The dictionary is required to be mutually incoherent, i.e., exhibit small mutual coherence as this is of significant importance for sparse reconstruction of signals [25, 26]. Fig. 5 shows that the mutual coherence between most of the dictionary elements is very small.

## 5. CONCLUSION

We have constructed an overcomplete multiscale dictionary of Slepian functions, which are solutions to the Slepian spatial-spectral concentration problem for bandlimited functions on the sphere, using hierarchical equal area iso-latitude iso-longitude pixelization (HEALLPix) of the sphere into sub-regions called pixels. HEALLPix has an inherent quaternary tree structure whose size and height are given in terms of the bandlimit of the signal. We have conducted numerical simulations on the span of the dictionary elements and their mutual coherence and have shown that the dictionary comfortably spans the space of bandlimited functions which are optimally (energy) concentrated within a pixel on the sphere with most of its elements exhibiting negligibly small mutual coherence. We consider the use of the proposed dictionary for sparse reconstruction, multi-resolution analysis, optimal filtering, feature extraction and denoising of spherical signals as potential research directions for future work.

## 6. REFERENCES


[1] R. Ng, R. Ramamoorthi, and P. Hanrahan, "Triple product wavelet integrals for all-frequency relighting," *ACM Trans. Graph.*, vol. 23, no. 3, pp. 477–487, Aug. 2004.

[2] T. S. Pollock, T. D. Abhayapala, and R. A. Kennedy, "Introducing space into MIMO capacity calculations," *J. Telecommun. Syst.*, vol. 24, no. 2, pp. 415–436, Oct. 2003.

[3] A. P. Bates, Z. Khalid, and R. A. Kennedy, "Novel sampling scheme on the sphere for head-related transfer function measurements," *IEEE/ACM Trans. Audio., Speech, Language Process.*, vol. 23, no. 6, pp. 1068–1081, Jun. 2015.

[4] W. Zhang, M. Zhang, R. A. Kennedy, and T. D. Abhayapala, "On high-resolution head-related transfer function measurements: An efficient sampling scheme," *IEEE Trans. Acoust., Speech, Signal Process.*, vol. 20, no. 2, pp. 575–584, 2012.

[5] A. P. Bates, Z. Khalid, and R. A. Kennedy, "An optimal dimensionality sampling scheme on the sphere with accurate and efficient spherical harmonic transform for diffusion mri," *IEEE Signal Process. Lett.*, vol. 23, no. 1, pp. 15–19, Jan. 2016.

[6] D. N. Spergel, R. Bean, O. Doré, M. R. Nolta, C. L. Bennett, J. Dunkley, G. Hinshaw, N. Jarosik, E. Komatsu, L. Page, H. V. Peiris, L. Verde, M. Halpern, R. S. Hill, A. Kogut, M. Limon, S. S. Meyer, N. Odegard, G. S. Tucker, J. L. Weiland, E. Wollack, and E. L. Wright, "Three-year Wilkinson Microwave Anisotropy Probe (WMAP) observations: Implications for cosmology," *The Astrophysical Journal Supplement Series*, vol. 170, no. 2, pp. 377–408, 2007.

[7] M. A. Wieczorek and F. J. Simons, "Minimum variance multitaper spectral estimation on the sphere," *J. Fourier Anal. Appl.*, vol. 13, no. 6, pp. 665–692, 2007.

[8] S. G. Mallat, "A theory for multiresolution signal decomposition: the wavelet representation," *IEEE Trans. Pattern Anal. Mach. Intell.*, vol. 11, no. 7, pp. 674–693, Jul. 1989.

[9] I. Daubechies, "The wavelet transform, time-frequency localization and signal analysis," *IEEE Trans. Inf. Theory*, vol. 36, no. 5, pp. 961–1005, Sep. 1990.

[10] S. G. Mallat, *A Wavelet Tour of Signal Processing*, 3rd ed. Massachusetts, USA: Academic Press, 2009.

[11] J. P. Antoine and P. Vandergheynst, "Wavelets on the 2-sphere: a group theoretical approach," *Applied Comput. Harm. Anal.*, vol. 7, pp. 1–30, 1999.

[12] Y. Wiaux, L. Jacques, and P. Vandergheynst, "Correspondence principle between spherical and euclidean wavelets," *Applied Comput. Harm. Anal.*, vol. 632, pp. 15–28, 2005.

[13] J. L. Starck, Y. Moudden, P. Abrial, and M. Nguyen, "Wavelets, ridgelets and curvelets on the sphere," *Astron. & Astrophys.*, vol. 446, pp. 1191–1204, Feb. 2006.

[14] B. Leistedt and J. D. McEwen, "Exact wavelets on the ball," *IEEE Trans. Sig. Proc.*, vol. 60, no. 12, pp. 6257–6269, 2012.

[15] A. P. Bates, Z. Khalid, and R. A. Kennedy, "Slepian spatial-spectral concentration problem on the sphere: Analytical formulation for limited colatitude-longitude spatial region," *IEEE Trans. Signal Process.*, vol. 65, no. 6, pp. 1527–1537, Mar. 2017.

[16] F. J. Simons, F. A. Dahlen, and M. A. Wieczorek, "Spatiospectral concentration on a sphere," *SIAM Rev.*, vol. 48, no. 3, pp. 504–536, 2006.

[17] A. P. Bates, Z. Khalid, and R. A. Kennedy, "Efficient computation of slepian functions on the sphere," *IEEE Trans. Signal Process.*, vol. 65, no. 16, pp. 4379–4393, Aug. 2017.

[18] R. A. Kennedy and P. Sadeghi, *Hilbert Space Methods in Signal Processing*. Cambridge, UK: Cambridge University Press, Mar. 2013.

[19] D. Slepian and H. O. Pollak, "Prolate spheroidal wave functions, Fourier analysis and uncertainity-I," *Bell Syst. Tech. J.*, vol. 40, pp. 43–63, Jan. 1961.

[20] H. J. Landau and H. O. Pollak, "Prolate spheroidal wave functions, Fourier analysis and uncertainity-II," *Bell Syst. Tech. J.*, vol. 40, pp. 65–84, Jan. 1961.

[21] D. Slepian, "Prolate spheroidal wave functions, fourier analysis and uncertainty – iv: Extensions to many dimensions; generalized prolate spheroidal functions," *Bell Syst. Tech. J.*, vol. 40, pp. 3009–3057, Jun. 1964.

[22] F. J. Simons and D. V. Wang, "Spatiospectral concentration in the cartesian plane," *Intern. J. Geo-math.*, vol. 2, pp. 1–36, 2011.

[23] M. A. Wieczorek and F. J. Simons, "Localized spectral analysis on the sphere," *Geophys. J. Int.*, vol. 162, no. 3, pp. 655–675, Sep. 2005.

[24] K. M. Górski, E. Hivon, A. J. Banday, B. D. Wandelt, F. K. Hansen, M. Reinecke, and M. Bartelmann, "HEALPix: A Framework for High-Resolution Discretization and Fast Analysis of Data Distributed on the Sphere," *Astrophys. J.*, vol. 622, pp. 759–771, Apr. 2005.

[25] J. A. Tropp and A. C. Gilbert, "Signal recovery from random measurements via orthogonal matching pursuit," *IEEE Trans. Inf. Theory*, vol. 53, no. 12, pp. 4655–4666, Dec. 2007.

[26] R. Gribonval and M. Nielsen, "Sparse representations in unions of bases," *IEEE Trans. Inf. Theory*, vol. 49, no. 12, pp. 3320–3325, Dec. 2003.